

Supporting Information:

Fluorescence blinking as an output signal for biosensing

Brandon Roark¹, Jenna A. Tan², Anna Ivanina¹, Morgan Chandler¹, Jose Castaneda¹, Ho Shin Kim³, Shriram Jawahar¹, Mathias Viard^{4,5}, Strahinja Talic¹, Kristin L. Wustholz², Yaroslava G. Yingling³, Marcus Jones^{1,6}, Kirill A. Afonin^{1,6*}*

¹ Department of Chemistry, University of North Carolina at Charlotte, 9201 University City Boulevard, Charlotte, North Carolina 28223, USA

² Department of Chemistry, College of William and Mary, Williamsburg, VA 23185, USA

³ Department of Materials Science and Engineering, North Carolina State University, Raleigh, North Carolina 27695-7907, USA

⁴ Gene Regulation and Chromosome Biology Laboratory, Center for Cancer Research, National Cancer Institute, Frederick, MD, USA

⁵ Basic Science Program, Leidos Biomedical Research, Inc., RNA Biology Laboratory, Frederick National Laboratory for Cancer Research, Frederick, MD 21702, USA

⁶ Nanoscale Science Program, University of North Carolina at Charlotte, Charlotte NC 28223, USA; The Center for Biomedical Engineering and Science, University of North Carolina at Charlotte, Charlotte NC 28223, USA.

Corresponding Authors

* To whom correspondence should be addressed:

Marcus Jones, phone 704-687-7852, e-mail: marcus.jones@uncc.edu;

Kirill A. Afonin, phone 704-6870685, e-mail: kafonin@uncc.edu;

Table of Contents:

S-1: Title Page

S-3: Oligo sequences used in this project

S-4 – S-7: Extended Material and Methods

S-9: Supporting Figure S1: Confocal Fluorescence Microscopy Images and Blinking Traces of Free QDs

S-10: Supporting Figure S2: Schematic Design Principles of Biosensor and QD Lattice Formations

S-11: Supporting Figure S3: Formation of QD lattices analyzed with agarose gel

S-12: Supporting Figure S4: Molecular Dynamics Simulations of Three-Stranded Complexes

S-13: Supporting Figure S5: Confocal Fluorescence Images of Biosensor with Target Incubated at 55 °C.

S-14: Supporting Figure S6: Confocal Fluorescence Microscopy Images and Corresponding Blinking Traces of Biosensor and Biosensor with Target at Different Incubation Temperatures and Ratios.

S-15: Supporting Figure S7: Binomial Probability Distribution of Different Number of QDs in the Lattice.

S-16: Supporting References

Sequences used in this project

Target mDNA for *K-ras* with codon 12 mutation (GGT to GAT)¹:

5'-GTAGTTGGAGCTGATGGCGTAGGCAAGAGTGCCTTGACGATACAGCTAATTCAG

Dummy Target mDNAs tested as negative control:

D1

5'-GGGAGATTTAGTCATTAAGTTTTACAATCCGCTTTGTAATCGTAGTTTGTGT

D2

5'-GGGATCTTTACCTACCACGTTTTGCTGTCTCGTTTGCAGAAGGTCTTTCCGA

Sensor for recognition of *K-ras* mRNA

Guard strand

5`-CTGAATTAGCTGTATCGTCAAGGCACTCTTGCCTACGCCATCAGCTCCAAC

Anti-guard strand

5`-BIOTIN- GTTGGAGCTGATGGCGTAGGCAAGAGTGCCTTGACGATA

DNA for anti-guard

5`-BIOTIN- TATCGTCAAGGCACTCTTGCCTACGCCATCAGC

Supporting Material and Methods

Sequence design and preparation: Single-stranded DNAs entering the composition of biosensors were designed as schematically shown in supporting Fig. S2. Correct assemblies were tested with NUPACK². The full list of sequences used in this work is found above. All oligos were purchased from Integrated DNA Technologies (IDT), Inc. and gel purified on a denaturing urea gel (PAGE) (8% acrylamide (29:1), 8M urea). The oligos were eluted from gel slices overnight at 4°C into buffer containing 300 mM NaCl, 10 mM Tris pH 7.5, and 0.5 mM EDTA. After precipitating oligos in two volumes of 100% ethanol, samples were rinsed with 90% ethanol, vacuum dried, and dissolved in double-deionized water (ddiH₂O). Concentrations were measured using a UV-Vis spectrophotometer (NanoDrop 2000). Extinction coefficients for all strands were provided by IDT.

Assemblies and biosensor analysis with Electrophoretic Mobility Shift Assays (EMSA). All duplexes were assembled as detailed elsewhere³. Briefly, DNAs at concentrations specified in the text were mixed in ddiH₂O and incubated in a heat block at 95°C for two minutes. Afterwards samples were removed from heat, and placed at room temperature. Hybridization buffer (89mM Tris-borate, pH 8.3 and 2 mM magnesium acetate) was added to the mixtures either prior to heating, or after the step at 95°C. All assemblies and re-association experiments were analyzed at 4°C on 7% (29:1) native polyacrylamide gels in the presence of 89 mM Tris-borate, pH 8.3 and 2 mM magnesium acetate. Gels were run for 2 h at 150 mA and stained with ethidium bromide (EtBr). Formation of QD-based lattices was analyzed at room temperature with 2% agarose gels with and without EtBr added to the gel. Bio-Rad™ ChemiDoc MP Imaging System (Bio-Rad, Hercules, CA, USA) was used to visualize QDs (set for 525 nm) and EtBr (set for 605 nm) stained nucleic acids.

As a target strand, short fragment of DNA with sequence identical to *K-ras* (with codon 12 mutation) mRNA fragment¹ was used. For biosensor, prepared duplexes (Guard +Anti-guard) were mixed with DNAs for anti-guard and incubated with target mDNA fragments of *K-ras* for 1h at different temperatures 20°C, 37°C, 45°C, 50°C and 55°C. All samples were analyzed with 7% (29:1) native-PAGE at 4°C as described above.

Titration of Quantum Dots (QDs) with ssDNA strands. 20 µL of 0.2 µM QDs (Qdot® 545 ITK™ Streptavidin Conjugate Kit, Thermofisher) Qdot® incubation buffer (provided by

manufacturer) were prepared. Biotinylated ssDNAs (e.g. Anti-guard) of indicated concentrations were prepared through a series of dilutions with QD incubation buffer. To get the different QD: DNA ratios (1:30, 1:20, 1:15, 1:12, 1:10, 1:8, 1:6, 1:4, 1:2), 2 μL of QDs were mixed with 2 μL of DNAs at: 6.0 μM , 4.0 μM , 3.0 μM , 2.4 μM , 2.0 μM , 1.6 μM , 1.2 μM , 0.80 μM , and 0.40 μM . Mixtures were incubated at 37°C for 20 min, then loaded onto a 2% agarose gel with EtBr. The gel was run for 20 min at 220 Volts. All gels were visualized with Bio-Rad™ ChemiDoc MP Imaging System).

Titration of Quantum Dots (QDs) with dsDNA strands. 20 μL of 0.2 μM QDs (Qdot® 545 ITK™ Streptavidin Conjugate Kit, Thermofisher) in incubation buffer (provided by manufacturer) were prepared. Biotinylated dsDNAs (Anti-guard/DNA for anti-guard) of indicated concentrations were prepared through a series of dilutions with QD incubation buffer. To get the different QD: DNA ratios (1:20, 1:15, 1:12, 1:10, 1:8, 1:6, 1:4, 1:2, 1:1), 2 μL of QDs were mixed with 2 μL of DNAs at: 4.0 μM , 3.0 μM , 2.4 μM , 2.0 μM , 1.6 μM , 1.2 μM , 0.80 μM , 0.40 μM , and 0.20 μM . Mixtures were incubated at 37°C for 20 min, then loaded onto a 2% agarose gel with EtBr. Free QDs and duplexes were loaded as controls. The gel was run and visualized as described above.

Kinetics Assay determining time points of lattice formation on mixing of QDs and biotinylated duplexes (Anti-guard/DNA for anti-guard). 20 μL of 0.2 μM QDs in incubation buffer were prepared and mixed with 20 μL of 2 μM of biotinylated duplex to obtain a total volume of 40 μL at time point zero. The mixture was incubated at 37°C and 4.0 μL were aliquoted and snap frozen on dry ice at each time point: 30 sec, 1 min, 2 min, 3 min, 5 min, 10 min, 15 min, 30 min, and 60 min. After 60 min, 1 μL of DNase was added and the mix was additionally incubated for 30 min at 37°C. 4.0 μL of the samples were loaded on 2% agarose gel with EtBr in reverse order, along with free QDs and duplexes as controls. The gel was run and visualized as described above.

Series of dilutions of pre-formed QD lattices to determine the lowest concentration of lattices suitable for visual assessment. QD lattices (1:20 ratio of QD: DNA duplex) were prepared as described above. Series of dilutions with incubation buffer were performed to get the following concentrations of DNAs: 2.50 μM , 1.25 μM , 0.625 μM , 0.313 μM , 0.0781 μM , 0.0391 μM , 0.0195 μM , 0.00976 μM , 0.00488 μM , and 0.00244 μM . Diluted samples (5 μL) were run and visualized as described above. The free QDs were used as the control.

Biotin Competing DNA Agarose Gel. Three samples were prepared (100 nM QDs : 1.5 μ M ssDNA (3), 100 nM QDs : 1 μ M duplex (2+3), and 100 nM QDs: 1 μ M duplex (2+3) in the presence of 50 μ M of biotin and incubated at 37.0°C for 20 min. Samples were analyzed on agarose gels as described above.

Analysis of biosensors. After incubation for 20 min of target strand and prepared biosensors (Guard/Anti-guard duplex and DNA for anti-guard) at different temperatures (20°C, 37°C, 45°C, 50°C, and 55°C), samples were incubated with QDs. Based on titration experiments, the optimal QD to Biosensor ratio was chosen to be 1:10 (1:6 and 1:15 ratios were also tested). Samples were incubated for 30 min at 37°C and run on a 2% agarose gel (89 mM Tris, 80 mM boric acid, 2 mM EDTA, and pH 8.3).

Melting Temperatures (T_m s). DNA biosensor duplexes (1+2), (2+3), and (1+4) were assembled at 2 μ M concentrations as described above. Subsequently, 10 μ L of 10X SYBR® Green II RNA gel stain (Thermofisher) were mixed with 10 μ L of 2 μ M DNA duplexes.⁴ The mix was incubated in the dark for 20 min to ensure the intercalation. All three duplexes were placed into a CFX96 Real-Time™ System coupled with a C1000 Touch™ Thermal Cycler (Bio-Rad™). A melting curve protocol was selected which ranged from 50.0°C-95.0°C, the plate was read every 0.2°C. The data was processed using OriginPro 2016™ data analysis software where $-d(\text{RFU})/dT$ was plotted as a function of temperature. The T_m was determined by the peak finding function in OriginPro 2016™ from each negative first derivative plot.

Confocal imaging. Two confocal fluorescence instruments were used in this study (at UNCC for data shown in Figures 4, 5 and S5; at CWM for data shown in Figures 1, S1, S6).

At UNCC: QD-biosensor solutions before and after incubation with target strands were prepared for confocal imaging by diluting 1 μ L by two or three orders of magnitude with incubation buffer and were kept on ice until the moment of deposition. Diluted solutions (20 μ L) were spin coated onto methanol cleaned 18 \times 18 mm coverslips (Ted Pella, Inc.) with use of a Chemat KW-4A spin coater under the following 2-stage spin setting of 2,500 rpm for 2 seconds (Stage 1) and 3,000 rpm for 30 seconds (Stage 2). Prepared coverslips were then mounted onto a Nano-PDQ375 x-y-z translation stage for laser scanning confocal microscopy. Excitation was provided by a PicoQuant PDL 800-B pulsed laser with a LDH Series 470 nm laser head at a 10 MHz repetition frequency and power of 1.15 μ W. Excitation pulses were coupled into a single-mode optical fiber, then directed to a 500 nm cutoff dichroic beam splitter before being focused

onto the sample by a Zeiss 100× 1.25 NA oil immersion objective lens. Fluorescence from the sample was collected through the same objective and directed toward a bandpass filter with a 45 nm width centered about 535 nm before reaching a flip mirror. Orientation of this flip mirror either directed fluorescence toward a Melles Griot 160/0.17 objective lens that focused the signal onto a EG & E Single Photon Counting Module (SPCM) for imaging, or to a Nikon 10× objective lens that focused signal onto a PicoQuant PDM Series Single Photon Avalanche Photodiode (SPAD) for collection of blinking dynamics.

Experimental control and data acquisition was achieved using a homebuilt LabVIEW program. Size and scanning rate for images was 512 × 512 pixels at 5 lines per seconds. ImageJ was used for image analysis. Detection signals from the SPAD were sent to a Time-Harp200 PCI Card operating in time tagged time-resolved mode, and blinking data were recorded for 180 seconds at each bright spot. Photon macro times were organized into 10 ms bins to yield blinking trajectories from which intensity histograms were produced.

At CWM: QD-biosensor solutions were spin coated onto methanol-cleaned glass coverslips (Fisher Scientific, 12-545-102) with the use of a spin coater (Laurell Technologies, WS-400-6NPP-LITE) under the following 2-stage spin setting of 2,500 rpm for 2 seconds and 3,000 rpm for 30 seconds. Samples were placed into a custom-built cell on a nanopositioning stage (Physik Instrumente LP E-545) atop an inverted confocal microscope (Nikon, TiU). Laser excitation was provided by a PicoQuant PDL 800-D pulsed laser with a LDH series 470 nm laser head at a 10 MHz repetition frequency and power of ~1.43 μW. Excitation pulses were then directed to a 488 nm cutoff dichroic beam splitter (Semrock, Di02-R488-25x36) before being focused onto the sample by a Nikon Plan Fluor 100 × 1.3 NA oil immersion objective lens. Epifluorescence from the sample was collected by the same objective, and spectrally filtered by an edge filter (Semrock, BLP01-488R-25). The resulting signal was focused onto an avalanche photodiode detector (APD) with a 50 μm aperture (MPD, PDM050CTB) for images and blinking dynamics. A homebuilt LabVIEW program controlled the nanopositioning stage in 100 nm steps and collected emission. Blinking dynamics were recorded for 180 seconds using a 10 ms integration time. Image J was used to analyze measured areas.

Molecular Dynamics (MD) Simulation. A three-stranded complex which is composed of Target, Guard DNA and Anti-guard DNA was built via nucleic acid builder in Discovery Studio 4.5 package⁵. The same approach was used to build a complex with truncated nucleic acids.

Initial structures of three-stranded complexes were similar to DNA triplex structures and three strands interacted with each other via base-base interactions. FF14SB force field was used for partial charges and geometrical parameters of DNA and RNA⁶. We used AMBER 14⁷ for MD simulations including minimization, heating, and production runs. The systems started from the minimization for 10,000 steps. In order to investigate temperature effect on DNA – RNA complex, we employed four different heating steps and each case was gradually heated up to 300 K, 328 K, 333K, and 368 K, respectively, for 200 ps using Langevin dynamics. After these systems were equilibrated and heated, production MD runs were performed for 30 ns with 2 fs time steps in implicit solvent condition⁸. Non-bonded interactions were analyzed using a combination of in-house scripts that have been used for protein α -helix and solvent interactions⁹ and NAMD energy in VMD 1.9.1 software¹⁰. All simulations snapshots were taken by VMD 1.9.1 software¹⁰.

Supporting Figures

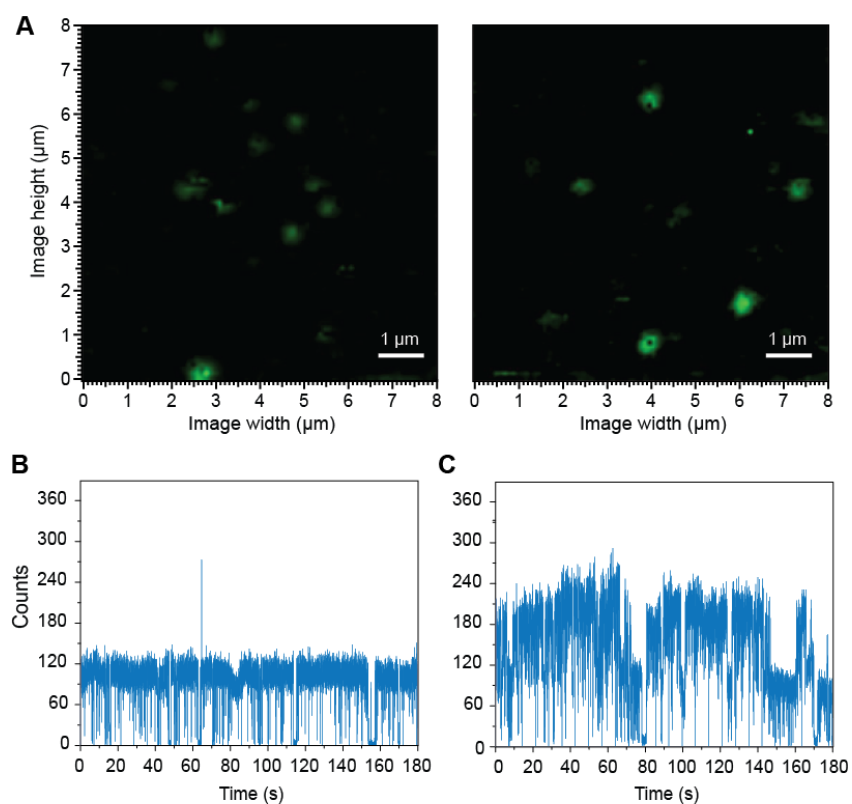


Figure S1. Representative QD fluorescence microscopy images (A) and blinking traces (B-C) of free QDs at 100 pM. (B) shows a representative blinking trace from an individual QD and (C) shows a representative blinking trace that can be attributed to a small QD aggregate. Of 27 QDs, 25 monomers (93%) were detected based on the observation of diffraction-limited spot size, binary blinking dynamics, and consistent emissive/non-emissive intensities.

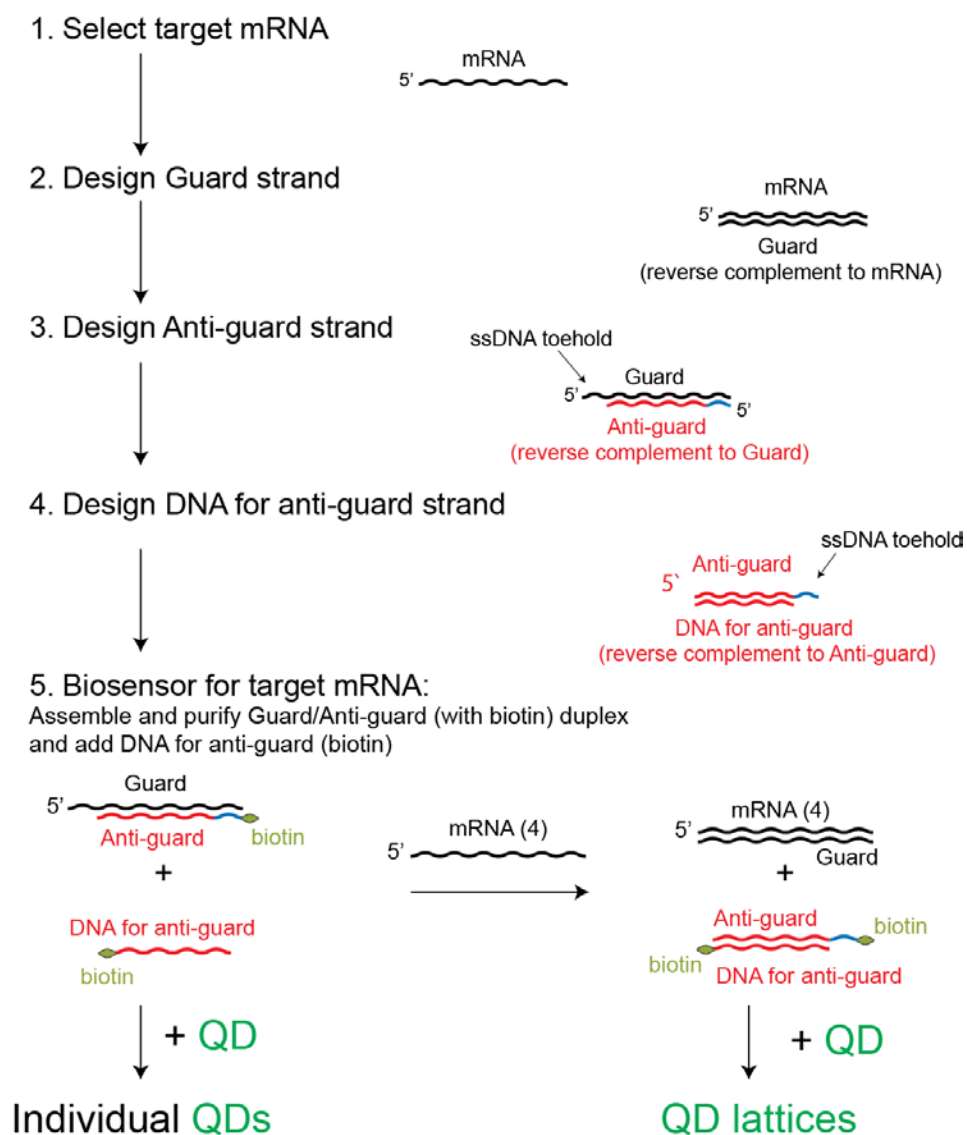


Figure S2. Schematic representation of the designing approach used in this work. The lengths of the toeholds were defined based on the re-association rules described elsewhere. The free energies of secondary structures were calculated to be -77 kcal/mol for duplex (1+2), -65 kcal/mol for duplex (2+3), and -97 kcal/mol for duplex (1+4). The difference of -12 kcal/mol prevents duplex (2+3) formation in biosensor set up ((1+2) +3). However, the presence of target strand makes the formation of (2+3) more favorable, by -85 kcal/mol, due to (1+4) association.

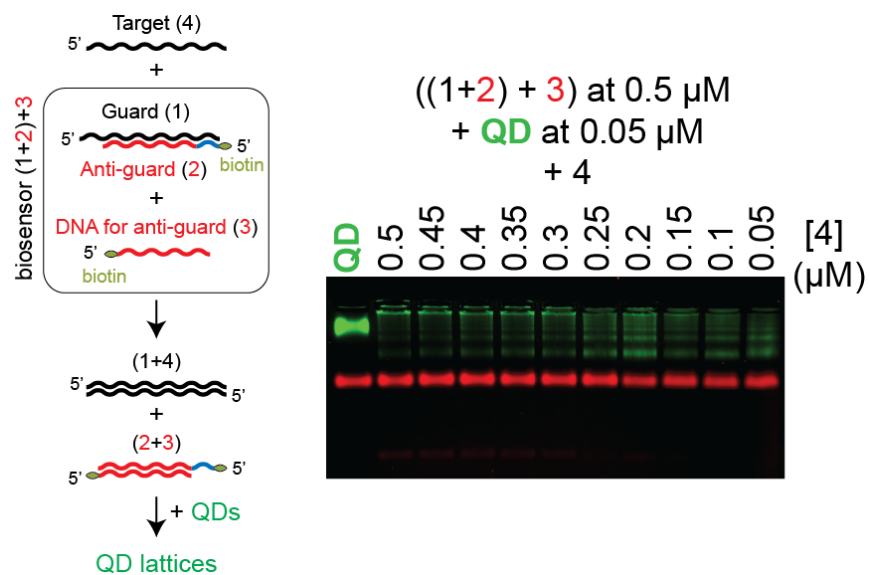


Figure S3. Formation of QD lattices. Titration experiments with different amounts of Target strand, at concentrations indicated on the gel, mixed with constant amounts of Sensor ((1+2)+3) at 0.5 μM . Concentration of QD was 50 nM in all samples. The panel on the left is the schematics explaining the working principle of biosensor and corresponding nomenclature.

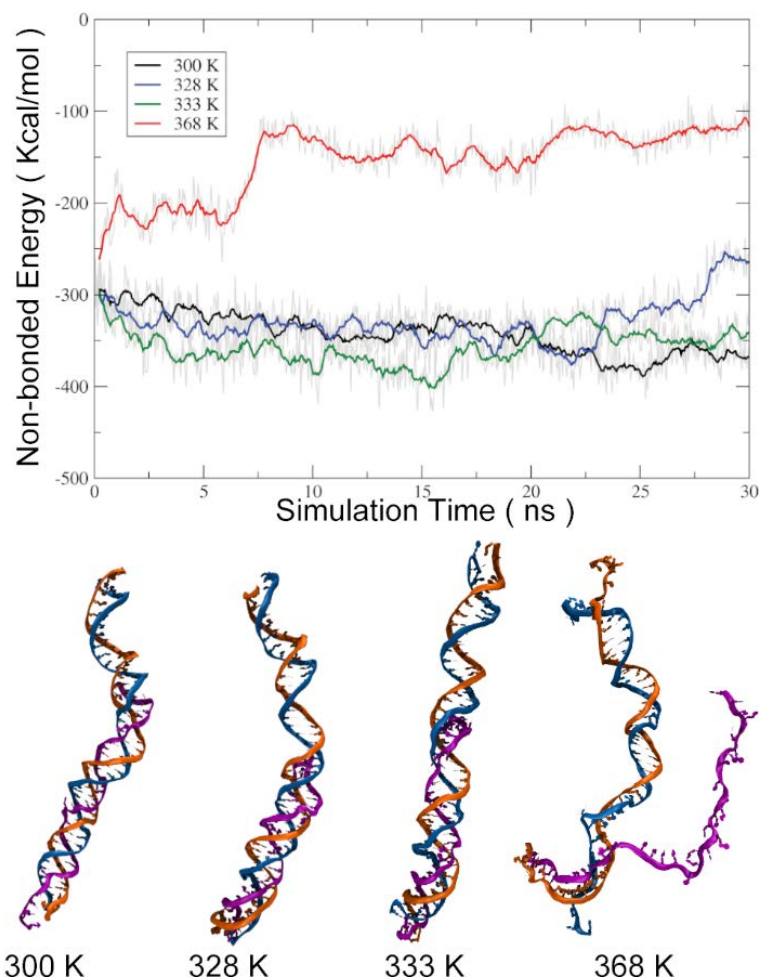


Figure S4. Temporal profile of non-bonded interactions between Anti-guard DNA (purple strand) and target (orange strand) – Guard DNA (blue strand) complex at 300 K (black), 328 K (blue), 333 K (green) and 368 K (red) and corresponding simulation snapshots. Simulation results, indicate that Anti-guard, target, and Guard strands may form stable complexes held together *via* strong internal non-bonded interactions at 27°C (300 K), 55°C (328 K), and 60°C (333 K). At a very high temperature of 95°C (368 K), however, the Anti-guard strand denatures from the complex followed by the loss of stability of target-guard interactions. Interestingly, initial structures between target-guard can be maintained efficiently even at 95°C due to strong non-bonded base-base pairing. The DINAmelt¹¹⁻¹² software predicts the melting temperature for target-guard complex as approximately 90.1°C, which agrees well with our observations.

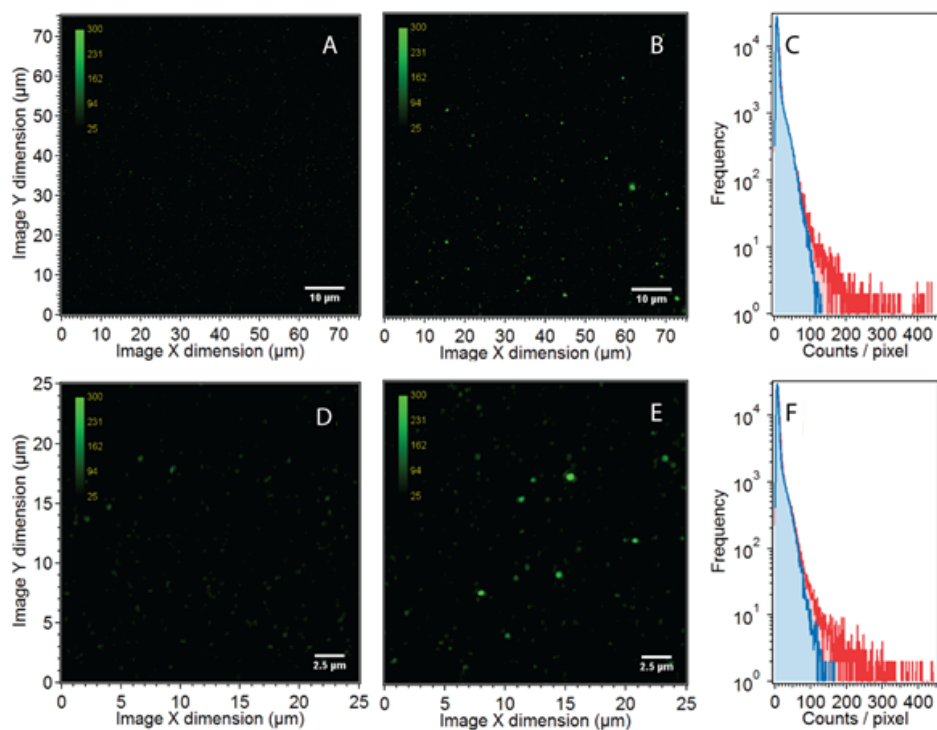


Figure S5. Fluorescence microscopy images of **A:** sensor + QDs and **B:** sensor + QDs (at 1:10 ratio), after incubation with target strands at 55°C. **C:** Intensity histograms for the images in **A** (blue) and **B** (red). Fluorescence microscopy images of 25 x 25 μm area of **D:** sensor + QDs and **E:** sensor + QDs after incubation with target strand at 55°C. **F:** Intensity histograms for the images in **D** (blue) and **E** (red).

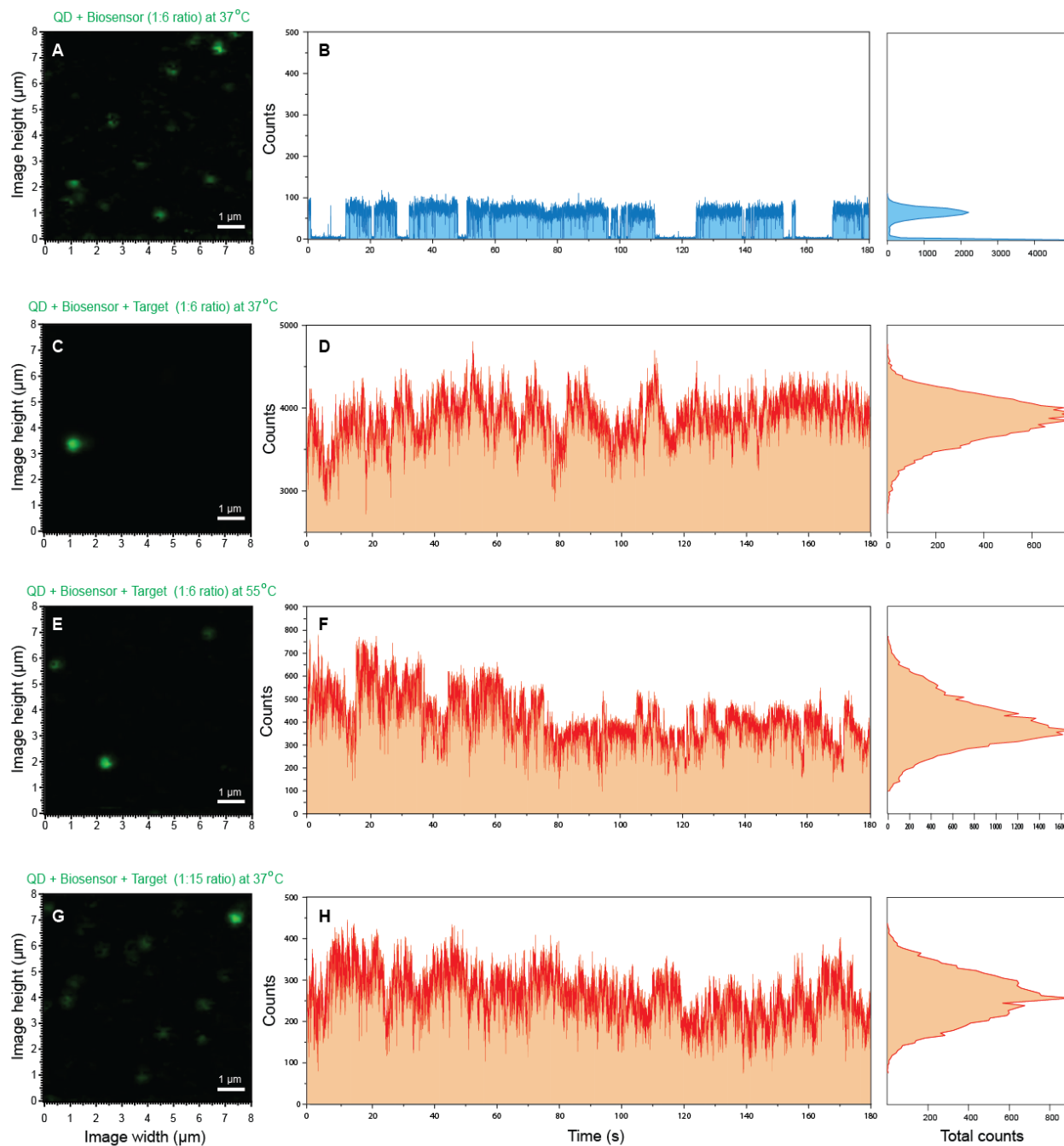


Figure S6. Fluorescence microscopy images and corresponding blinking traces of **A-B:** QDs + sensor (at 1:6 ratio), **C-D:** QDs + sensor (1:6) after incubation with target strands at 37°C, **E-F:** QDs + sensor (1:6) after incubation with target strands at 55°C measured, and **G-H:** QDs + sensor (1:15) after incubation with target strands at 37°C. All samples were analyzed at 800 pM concentration.

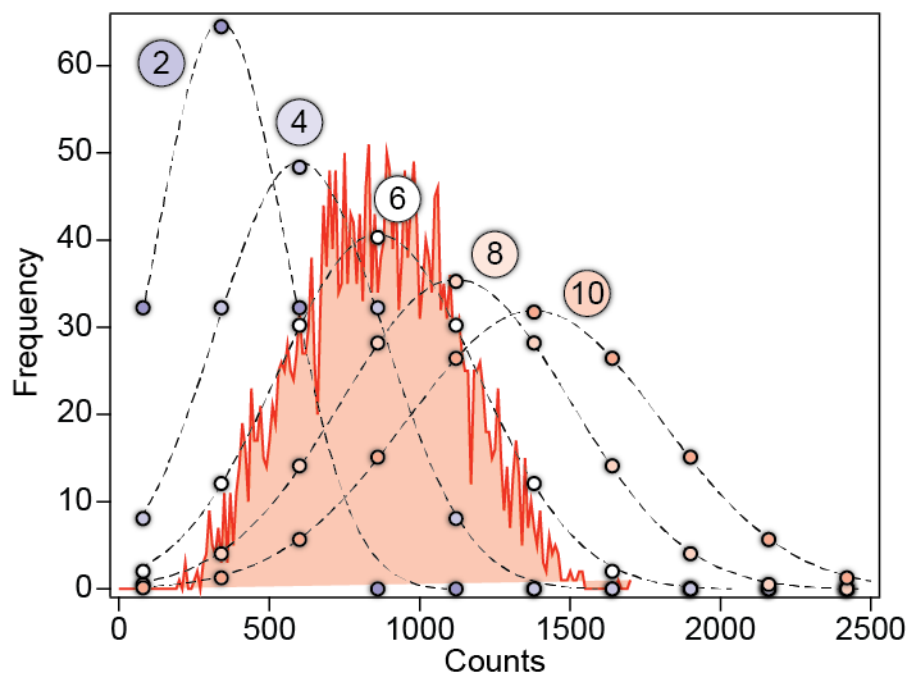


Figure S7. Binomial probability distributions illustrating the likelihood of finding 2, 4, 6, 8, and 10 QDs in the QD lattice from Figure 5D. Intensities are derived from the intensity of single QD emission shown in Figure 5C.

Supporting References

1. (a) Kam, Y.; Rubinstein, A.; Nissan, A.; Halle, D.; Yavin, E., Detection of endogenous K-ras mRNA in living cells at a single base resolution by a PNA molecular beacon. *Mol Pharm* **2012**, *9* (3), 685-93; (b) Minamoto, T.; Mai, M.; Ronai, Z., K-ras mutation: early detection in molecular diagnosis and risk assessment of colorectal, pancreas, and lung cancers--a review. *Cancer detection and prevention* **2000**, *24* (1), 1-12.
2. Zadeh, J. N.; Steenberg, C. D.; Bois, J. S.; Wolfe, B. R.; Pierce, M. B.; Khan, A. R.; Dirks, R. M.; Pierce, N. A., NUPACK: Analysis and design of nucleic acid systems. *J Comput Chem* **2010**, *32* (1), 170-3.
3. Afonin, K. A.; Viard, M.; Martins, A. N.; Lockett, S. J.; Maciag, A. E.; Freed, E. O.; Heldman, E.; Jaeger, L.; Blumenthal, R.; Shapiro, B. A., Activation of different split functionalities on re-association of RNA-DNA hybrids. *Nature nanotechnology* **2013**, *8* (4), 296-304.
4. Li, H.; Zhang, K.; Pi, F.; Guo, S.; Shlyakhtenko, L.; Chiu, W.; Shu, D.; Guo, P., Controllable Self-Assembly of RNA Tetrahedrons with Precise Shape and Size for Cancer Targeting. *Advanced Materials* **2016**, *28* (34), 7501-7507.
5. BIOVIA, D. S. *Discovery Studio Modeling Environment*, Release 4.5; Dassault Systèmes: San Diego, 2015.
6. Maier, J. A.; Martinez, C.; Kasavajhala, K.; Wickstrom, L.; Hauser, K. E.; Simmerling, C., ff14SB: Improving the Accuracy of Protein Side Chain and Backbone Parameters from ff99SB. *J Chem Theory Comput* **2015**, *11* (8), 3696-3713.
7. D.A. Case, J. T. B., R.M. Betz, D.S. Cerutti, T.E. Cheatham, III, T.A. Darden, R.E. Duke, T.J. Giese,; H. Gohlke, A. W. G., N. Homeyer, S. Izadi, P. Janowski, J. Kaus, A. Kovalenko, T.S. Lee, S. LeGrand,; P. Li, T. L., R. Luo, B. Madej, K.M. Merz, G. Monard, P. Needham, H. Nguyen, H.T. Nguyen, I.; Omelyan, A. O., D.R. Roe, A. Roitberg, R. Salomon-Ferrer, C.L. Simmerling, W. Smith, J. Swails,; R.C. Walker, J. W., R.M. Wolf, X. Wu, D.M. York and P.A. Kollman *AMBER 2015*, University of California: San Francisco, 2015.
8. Bashford, D.; Case, D. A., Generalized born models of macromolecular solvation effects. *Annu Rev Phys Chem* **2000**, *51*, 129-152.
9. Kim, H. S.; Ha, S. H.; Sethaphong, L.; Koo, Y. M.; Yingling, Y. G., The relationship between enhanced enzyme activity and structural dynamics in ionic liquids: a combined computational and experimental study. *Phys Chem Chem Phys* **2014**, *16* (7), 2944-2953.
10. Humphrey, W.; Dalke, A.; Schulten, K., VMD: Visual molecular dynamics. *Journal of Molecular Graphics & Modelling* **1996**, *14* (1), 33-38.
11. Markham, N. R. & Zuker, M. (2005) DINAMelt web server for nucleic acid melting prediction. *Nucleic Acids Res* **2005**, *33*, 577-581.
12. Markham, N. R. & Zuker, M. (2008) UNAFold: software for nucleic acid folding and hybridization. In Keith, J. M., editor, *Bioinformatics, Volume II. Structure, Function and Applications*, number 453 in *Methods in Molecular Biology*, chapter 1, pages 3–31. Humana Press, Totowa, NJ. ISBN 978-1-60327-428-9.